



UNIVERSITY OF TWENTE.

Faculty of Science and Technology

Cytodex-3 microcarrier particle suspensions as bioactive embedding baths for 3D bioprinting

Lennart A. van Hoorne
Bachelor Thesis
Juli 2021

Supervisors:

Dr. Ir. J. Rouwkema

Msc. V. Trikalitis

External committee members:

prof.dr. J. Prakash

Vascularization lab
Department of Biomedical Engineering

BE-820

University of Twente

P.O. Box 217

7500 AE Enschede

The Netherlands

Abstract

Due to recent advancements in 3D bioprinting, creating large biological structures with high metabolic demands is becoming more and more of a reality. This calls for the need for pre-vascularized tissue. In this research, a novel printing technique will be used where printing is done inside a granular medium consisting of Cytodex-3 microparticles. Because of the nature of the granular medium, a 2,5D cell culture environment is created to stimulate arteriogenesis. The parameter used to manipulate the behavior of the granular medium is the volume fraction (V_f). The V_f is defined as the fraction of the total volume occupied by the microparticles. The goal of this research is to find the ideal V_f in which printing in the granular medium can be performed. First, the Cytodex-3 microparticles will be characterized in shape and size. Secondly, different granular mediums ranging from 50% to 70% V_f will be analyzed at macro and microscale. The third step will be to find an operational window for printing in the granular medium. With these results, Human Umbilical Vein Endothelial Cells (HUVECs) and Smooth Muscle Cells (SMCs) single cells and spheroids will be printed in a granular medium with the optimal V_f . Cytodex-3 microparticles are found to be spherical with an average diameter of $212 \pm 26 \mu\text{m}$ and a polydispersity of 0.54. Furthermore, the operational window for printing was found to be very large ranging from 55% to 65% V_f . If the V_f reached 70% it loses its self-healing property. Printing was done with a $410 \mu\text{m}$ nozzle, so lines were compared to this inner diameter. Best print resolutions were found at $677 \pm 120 \mu\text{m}$ and $531 \pm 90 \mu\text{m}$ for 60% and 65% respectively. Due to time constraints, cell printing is not yet performed successfully, but it is recommended to test this during future experiments because of promising results obtained during this research.

keywords: 3D-bioprinting, Granular Medium, Volume fraction, Cytodex-3, Vascularization

Acknowledgements

I want to thank the Vascularization Lab for their hospitality during this thesis. In particular, I want to thank Vasileios Trikalitis for his continued support these past few weeks. He showed me how to properly conduct research and with that the importance of being methodical when doing it. I also want to thank Vincent Rangel for always being quick to respond when I had any questions and showing me around all the labs. Last but not least, I want to thank Kees Wuister for working together these past few weeks. He helped me see solutions I would have trouble finding otherwise. I also want to thank the committee (MSc V. Trikalitis, Dr. Ir. J. Rouwkema and prof. dr. J. Prakash) for taking their time to read and judge this thesis.

Lennart van Hoorne
Enschede, 12 Juli, 2021

Contents

Abstract	ii
Acknowledgments	iii
1 Introduction	1
1.1 Countering the limitations of bioprinting	2
1.2 The need for pre-vascularized tissue	3
1.3 2,5D cell culture: bridging the gap between 2D en 3D cell culture	3
1.4 Research goal	4
2 Materials and Methods	5
2.1 Materials	5
2.1.1 Cytodex-3	5
2.1.2 3D-printer	6
2.1.3 Xanthan gum with blue fluorescent particles	6
2.1.4 PDMS bioreactor	7
2.1.5 Cell-laden bioink	7
2.1.6 Imaging	8
2.2 Methods	9
2.2.1 Determining the diameter of the Cytodex-3 beads	9
2.2.2 Embedding baths	9
2.2.3 Volume fraction	9
2.2.4 Creating the Cytodex-3 suspension	10
2.2.5 Creating the PDMS bioreactor	10
2.2.6 Analysing the self-healing properties of the suspension	11
2.2.7 Printing with xanthan gum	11
2.2.8 Printing with cell-laden bio-ink	11
2.2.9 Protocol cell culture	12
2.2.10 Protocol spheroid culture	13
3 Results	14
3.1 The characterization of Cytodex	14
3.1.1 Partly saturated	14
3.1.2 Fully saturated	15
3.2 Volume fraction and 3D printing: Establishing the operational window	16
3.2.1 Different volume fractions: Macro vs. Micro	16
3.2.2 Determining print resolutions	17
3.2.3 Print resolution vs. Volume fraction	19
3.2.4 The complete line	19
3.3 Cell printing	20

4 Discussion	21
5 Conclusion	23
A Abstract Nederlands	27
B G-code	28

Chapter 1

Introduction

3D printing, or additive manufacturing, is a rapid prototyping technique where a print-head creates a 3D object by, for example stacking 2D layers on top of each other. The 3D printer was originally commercialized in 1980 [1] and shows great potential due to its high accuracy, rapid prototyping and the ability to create complex structures [2, 3]. 3D bioprinting is used in the field of tissue engineering to precisely position biological materials to fabricate 3D structures [4]. As of today, there are three techniques used in 3D-bioprinting: Inkjet bioprinting, microextrusion bioprinting and laser-assisted bioprinting [4]. The different techniques can be seen in figure 1.1.

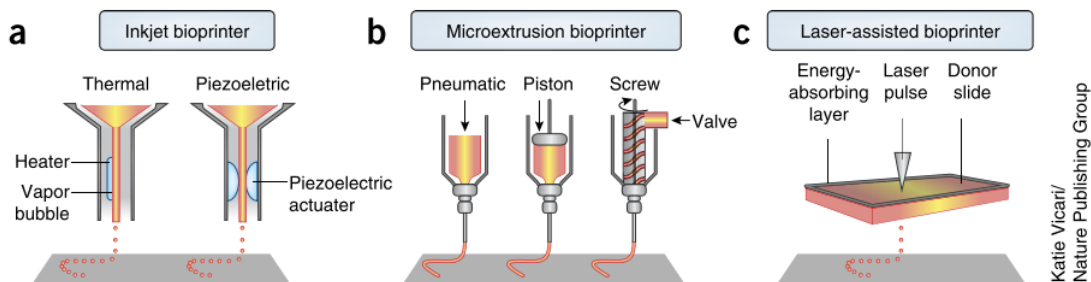


Figure 1.1: Different 3D bioprinting techniques [4]

Inkjet printing is a technique where controlled volumes of liquid are placed in a predefined location. Via thermal or acoustic cues droplets are placed onto a substrate, which supports or can become part of the final object [4]. Advantages of inkjet printing are low cost, high cell viability and the ability to print in high resolution [5]. In figure 1.1b you can see the second technique used, microextrusion bioprinting. Microextrusion uses pneumatic or mechanical systems to extrude a continuous line of bio-ink [6, 7]. Extrusion printing is the most used technique in non-biological 3D printing [4]. The last technique is laser-assisted bioprinting (LAB). Out of these three bioprinting techniques, LAB is the least used [4]. LAB is based on laser-induced forward transfer to enable precise printing of individual cells. Although LAB can reach high accuracy its drawbacks are high costs and low flow rates [6].

1.1 Countering the limitations of bioprinting

3D printing was originally designed to work with ceramic and plastic and the process usually involved organic solvents, high temperature and cross-linking agents that are not compatible with living cells. This makes the choice of materials one of the largest problems when working with bioprinting [8]. Next to this, the mechanical forces caused by the extrusion of ink are thought to reduce cell viability [4, 9].

Since the materials used in 3D-bioprinting need to be gelled and supported during printing because of the mechanical nature of the materials, it is hard to print complex structures[4]. To overcome this limitation different approaches have been tried including sacrificial layer techniques[10, 11] and Freeform Reversible Embedding of Suspended Hydrogels (FRESH)[12]. FRESH makes use of a hydrogel support bath in which a second hydrogel is printed. The bath then supports this hydrogel allowing it to maintain its form. The support bath, consisting of gelatin microparticles, is removed afterward by raising the temperature to 37 degrees Celsius.

Whereas FRESH uses two hydrogels, Bhattacharjee T et al. introduces a new technique where a granular medium is used as a support bath [13]. They show that as the tip moves, the granular gel locally fluidizes due to the shear stress applied by the tip and then rapidly solidifies, leaving space for the ink to be placed. This enables complex structures to be made with high precision shown in figure 1.2. Besides the ability to print with high precision, the self-healing property makes it possible to print in places where the needle has already passed[13].

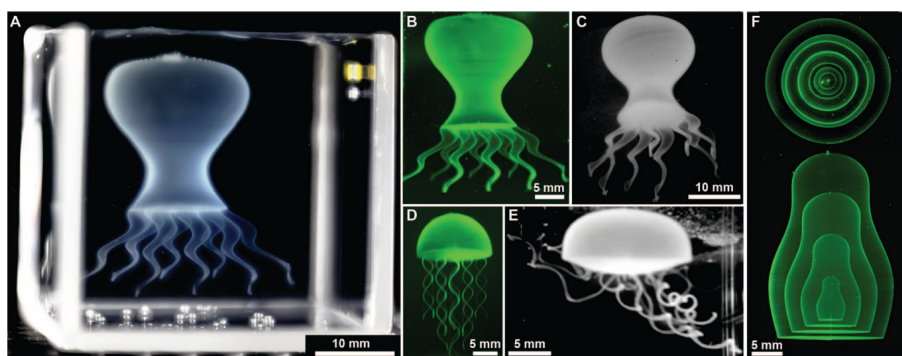


Figure 1.2: High precision printing by writing in the granular medium [13]

1.2 The need for pre-vascularized tissue

Due to the recent advancement in 3D bioprinting, creating large biological structures with high metabolic demand is becoming more and more a reality [9, 14]. This calls for the need for pre-vascularized tissue [14, 15]. Two main problems arise because of this. Awwad et al. have shown that the maximum spacing between capillary systems is $300\ \mu\text{m}$ otherwise causing nutrition limitations[16] and due to high consumption of oxygen in growing cells, hypoxia lurks around the corner[15]. When an implant with the size of a few hundred millimeters is implanted, the host will invade the implant creating blood vessels, which means that cells far from the host experience nutrient limitations eventually presenting a necrotic core [14]. An example of a successful study is a study by Chen et al. where gelMA is used to create a 3D environment enabling vascular paths to grow using human blood-derived endothelial colony-forming cells (ECFCs) and bone marrow-derived mesenchymal stem cells (MSCs)[17]. Other examples of techniques used to increase vascularization are microfabrication, growth factors, microsurgery, co-culture or a combination of these techniques [18].

1.3 2,5D cell culture: bridging the gap between 2D en 3D cell culture

2D cell culture has been used for the past century and has given us great insights into cell response to biochemical and physical cues [19]. Still, recent studies have investigated the possibility of 3D cell culture due to its close resemblance to the *in vivo* situation [20]. However, problems have been shown when culturing in 3D due to lack of mechanical cues [21]. 2,5D tissue culture has therefore been introduced, trying to combine both ways of cell culture [21]. For this reason, 2,5D tissue culture environment has been gaining more and more attention in the last decade [22, 23, 24]. In figure 1.3 an example can be found of 2,5D tissue culture compared to the more traditional 2D and 3D cell culture of fibroblasts. In this particular case between two hydrogel layers [21]

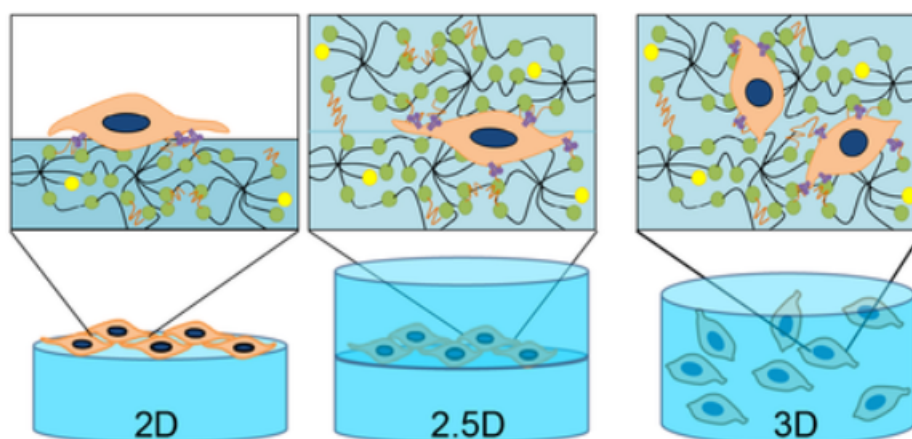


Figure 1.3: An example of a 2,5D culture of fibroblasts [21]

1.4 Research goal

The aim of this thesis is to combine the topics discussed in the introduction. This is done by creating a 3D bioprint environment by using a Cytodex-3 microbead suspension in which cells can attach to create a 2,5D cell culture environment. To achieve this, the following milestones will be addressed:

1. The characterization of the Cytodex-3 microbeads
2. Finding the operational window for printing
3. Printing of cells in a Cytodex-3 microbead suspension
4. Printing of spheroids in a Cytodex-3 microbead suspension

Given the limited time of this thesis, the goal is to at least complete the first two milestones to create a path for further research.

Chapter 2

Materials and Methods

2.1 Materials

This chapter will contain all equipment used and their specifications. As well as the materials used for printing and making the embedding baths.

2.1.1 Cytodex-3

Cytodex-3 is a dry powder surface microcarrier that is used for cell growth in suspension culture. Cytodex-3 is formed by coupling a layer of denatured collagen to a crosslinked dextran matrix[25]. The structure of Cytodex-3 can be seen in figure 2.1. In this thesis, Cytodex-3 beads are the microparticles that make up the embedding bath. Due to its wide use in tissue engineering and the fact that they are gelatin layered beads, the hypothesis is that the cells will be able to attach to these microparticles creating the 2,5D environment mentioned earlier. The amount of beads/g is assumed at approximately 3 million beads[25]. This will later be important when producing the embedding baths.

Cytodex 3. Collagen layer coupled to surface.

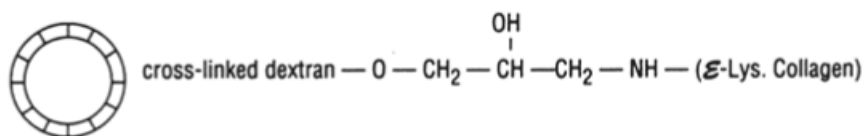


Figure 2.1: Chemical structure Cytodex-3 [25]

2.1.2 3D-printer

The printer used for bioprinting is a ROKIT INVIVO bioprinter. It is capable of printing freeform cell suspensions, hydrogels, thermoplastic filaments, pastes, and other composite materials, enabling both hard and soft tissue engineering [26]. The printer has two heads that can both extrude bio-ink simultaneously using the microextrusion technique [26, 7]. The syringes in which the bio-ink is loaded have a total volume of 1 mL (BD 1 mL luer lock).

Different diameter nozzles (Cellink) which are compatible with the luer lock syringe can be used ranging from an inner diameter of 51 - 514 μm . The printer is equipped with an H14 - HEPA filter, UV-C led, Chamber temperature display, HD camera and a bio-ink warmer making it perfect for bioprinting (See figure 2.2). Unlike many other 3D-printers, the printhead can only move in the z-direction whilst the bed moves in the x- and y-direction.

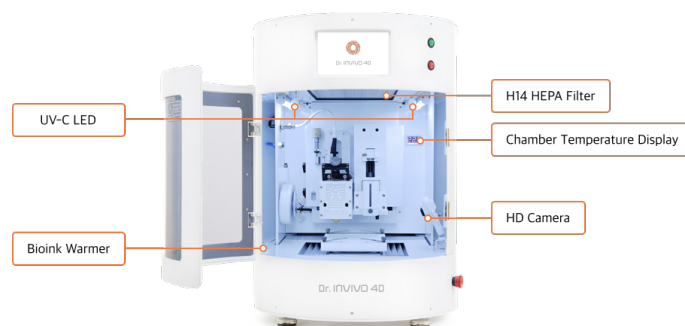


Figure 2.2: DR. INVIVO 4D2: The bioprinter used for printing

2.1.3 Xanthan gum with blue fluorescent particles

To show print resolution in different volume fractions, a straight line was printed with 1.5 % (w/v) xanthan ink filled with transparent ultramarine blue airbrush color (Createx Colors). The Xanthan was prepared by the Vascularization Lab. Xanthan is an extracellular polysaccharide that is secreted by the microorganism *Xanthomonas campestris* [27]. Xanthan is highly soluble in water, stable over a wide range of temperatures, acidic and alkine conditions. On top of that, it also has a low production cost. Because of these properties, it has been widely used in a variety of applications [28]. Examples of these applications are advanced drug delivery, wastewater treatment, protein delivery, tissue engineering, and food packing [29]. Furthermore, it is a cheap and stable way of testing print resolutions in different volume fractions.

2.1.4 PDMS bioreactor

To monitor cell growth a bioreactor was made out of Polydimethylsiloxane (PDMS). PDMS was used because of its many favorable properties. It has a surface that has a low interfacial free energy, it is chemically inert, has good gas permeability and good thermal stability, and is optically transparent [30]. Since the compartments needed to be closed for it to be a bioreactor, a complementary lid was made. The compartments of the bioreactor have a total volume of 700 μL and are illustrated in figure 2.3 and 2.4.

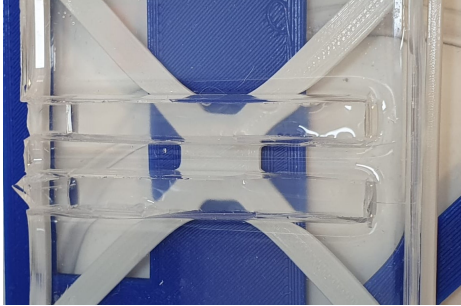


Figure 2.3: Bioreactor on the bed of the 3D printer

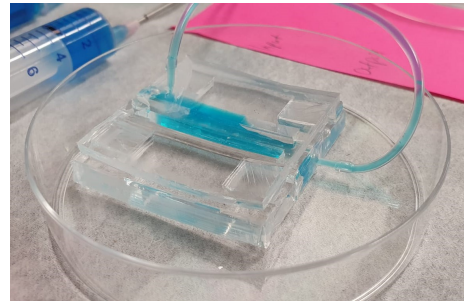


Figure 2.4: Complete bioreactor

2.1.5 Cell-laden bioink

When printing with cells, a cell-laden bio-ink was used containing Human Umbilical Vein Endothelial Cells (HUVEC), Smooth Muscle Cells (SMC) (1:1), Optiprep (Stemcell) and 1:1 SMC:HUVEC culture medium.

HUVECs

Endothelial cells have become a central theme in vascular research because it produces many different vasculoregulators and vasculotropic molecules which stimulate vascular growth [31]. HUVEC models greatly represent the physiological representation of the human vascular endothelium making it suitable for co-culture with SMCs [32]. The HUVECs were cultured in 88.5 % α -MEM, 10 % FBS, 2mM L-glutamin, 0.2 mM Ascorbic acid and 1x pen/strep.

SMCs

As mentioned in the last paragraph SMCs are very well suited for co-culture with HUVECs. Furthermore, SMCs are a promising cell therapy to promote angiogenesis [33]. The SMCs were cultured in 76.5 % DMEM (Thermo Fisher), 25 mM HEPES, 1x diluted pen/strep, 10 % Fetal Bovine Serum (FBS, Thermo Fisher) and 10 % Human serum (Thermo Fisher).

Optiprep

Optiprep is a density gradient medium used for specific cell isolation from whole blood making use of the density differences of the various leukocytes and the density gradient medium [34]. In the bio-ink, it is used as a medium to stop sedimentation of the cells.

2.1.6 Imaging

For imaging, the EVOS Microscope (Invitrogen EVOS FL Imaging System - Thermo fisher Scientific) is used. The microscope is able to both make images with transmitted light and fluorescent light. This makes it perfect for particle analyses as well as finding print resolution when using blue fluorescent particles. Aside from pictures a video recording device was used. This was especially useful when capturing the effect of different particles on the self-healing properties of the suspension.

2.2 Methods

All methods used in this thesis will be discussed in the following section.

2.2.1 Determining the diameter of the Cytodex-3 beads

Due to the round nature of Cytodex-3 beads, the diameter can be found using the equations 2.1 and 2.2.

$$A = \pi \times r^2 \quad \longrightarrow \quad r = \sqrt{A/\pi} \quad (2.1)$$

$$Diameter(d) = 2 \times r \quad (2.2)$$

By taking a large sample size, a histogram can be created to determine a probability density function. If this is a Gaussian function a mean diameter can be found, which in turn can be used to calculate the volume fraction. The polydispersity was found by taking the smallest particle (d) divided by the largest particle (D) ($\frac{d}{D}$) [35].

2.2.2 Embedding baths

Printing will be done in an embedding bath consisting of a Cytodex-3 particle suspension. The liquid will be milliQ in case of a non-cell experiment and in case of cell experiments this liquid will be 1:1 HUVEC/SMC medium. The most important property of the embedding bath should be that it is self-healing, meaning that when a needle runs through, the particles will afterward reconfigure to a position comparable to the initial position. The embedding bath will also be the 2,5D cell culture environment as described in the introduction. When the bio-ink is printed in the suspension, the cells hopefully attach to the microparticles creating a situation where not only the cells communicate with the surface of the microparticles but also the adjacent particles in the suspension. This might mimic an *in vivo* situation enabling the cells to communicate with each other to stimulate arteriogenesis.

2.2.3 Volume fraction

The key parameter to influence the behavior of the embedding bath is the volume fraction (V_f). The V_f is defined as the fraction of the total volume occupied by the beads[36]. In case the V_f is low, the suspension will behave more like a liquid. In case the V_f is high the suspension will behave more like solid.

This means V_f plays a heavy role in phase behavior. It has been found that for a V_f of 49% the suspension will behave like a fluid. Adding additional particles, in other words, raising the V_f , will crowd the suspension eventually reaching a fluid-crystal phase. A full crystal phase is reached at a V_f of 54% [35]. The next phase change is at 58% where the suspension reaches a glass phase, a solid with a fluid-like structure[37]. The maximum packing is reached at 74% V_f , which is also called tight packing[35].

The equation to determine the V_f is shown in equation 2.3 where r is the radius of the bead and n the number density, which can be found by dividing the number of colloidal particles by the total volume. [35].

$$V_f = \frac{4\pi r^3}{3}n \quad (2.3)$$

This essentially means that by knowing the radius of the particles, which is found in 3.1, and the number of particles in the suspension, the V_f can be estimated.

2.2.4 Creating the Cytodex-3 suspension

To create the different suspensions, first, a stock solution was made which can be extruded from a syringe. The key is to get this solution just right. When the solution is too diluted it will flow out of the syringe in an uncontrolled way. On the other hand, when the solution is too solid, the Cytodex-3 will not be distributed evenly. The right ratio was found at 11 $\mu\text{L}/\text{mg}$.

The stock solution is made in a 10 mL syringe. Before placing the Cytodex-3 inside the compartments it is first transferred into a 1 mL syringe for better accuracy. From the syringe, a predetermined amount of volume was added in the compartment. Since the ratio in the syringe is known. An approximation of the number of beads in the compartment can be made, which in turn can be used to calculate the V_f .

2.2.5 Creating the PDMS bioreactor

A compartment was made to hold the embedding baths. This was done by first laser cutting a mold out of Poly Methyl Methacrylate (PMMA) using a speedy 400 laser cutter (trotec). These parts were then fused using acetone. The protocol describes both the production of PDMS and the curing of the PDMS bioreactor.

Production of PDMS stock

1. Mix 45 g (9/10) of elastomer base in a tube + 5 g (1/10) of Curing agent together with the Base
2. Mix the two components for 5-6 minutes until air bubbles are totally embedded in the mixture
3. Put the bottle in the vacuum chamber for 20-40 minutes, such that all the air bubbles will vanish.
4. Remove the PDMS from vacuum bell.
5. Store the PDMS stock in the freezer, stock can be used for 3 months

Curing of the PDMS bioreactor

1. Place a microscopy glass slide necessary for imaging and the mold in a petri dish so that the glass is directly under the compartment
2. Fill the petri dish with prepared PDMS
3. Check again if the glass is still directly under the mold, if not reposition it correctly
4. Place the mold in the vacuum chamber for 20 minutes to remove bubbles
5. Check if the bubbles around the compartments are removed
6. Cure for 48 hours at room temperature so the compartment will cure homogeneously
7. Place in the oven at 65 degrees Celsius overnight
8. Cut off the petri dish from the PDMS
9. Cut away excess PDMS so only the bioreactor remains

2.2.6 Analysing the self-healing properties of the suspension

To capture the self-healing property of the suspension, videos were made of a needle running through the suspension. In preparation, 5 wells of a 24-well plate were filled to a final volume of 700 μL with V_f ranging from 50% to 70% with a 5% increment. The needle used was a 410 μm nozzle which is also used for printing.

2.2.7 Printing with xanthan gum

Before printing, embedding baths were prepared in the bioreactors with a final volume of 700 μL and V_f ranging from 50% to 70% with 5% increment. The xanthan gum was able to be loaded directly in the syringe for printing. before each print, the syringe is loaded for direct extrusion of the ink. Furthermore, the z-axis is calibrated so printing was done at a height that made it possible for the particles to be examined under the microscope. After printing, results were examined using the microscope with both translucent light, as well as a DAPI filter ($\lambda = 405 \text{ nm}$). Line width was determined using ImageJ and a full line picture was made using Inkscape.

2.2.8 Printing with cell-laden bio-ink

When printing with bio-ink, more preliminary steps need to be taken since the environment needs to be sterile. To achieve this, the bioreactors are autoclaved before use. The whole interior is cleaned with ethanol (70%) and the UV-C lamp is turned on one hour prior to printing. Embedding baths are made in a sterile environment with an optimal V_f found in the previous experiments. For the bio-ink, a cellular concentration was used of 10^6 cells/mL. After adding 5×10^6 of each cell type the suspension was centrifuged at 1000 rpm for 3 minutes. Supernatant was removed and 12% optiprep (stemcell) was added. After resuspending, the bio-ink was loaded into the syringe. All steps are performed inside a LAF-cabinet to minimize chance of infection. When transporting the syringe to the printer, a stopper (luer lock) is attached to maintain a closed environment. From this point, the same steps were taken as described in section 2.2.7.

After printing, the bioreactors must be placed under the microscope for day-0 examination. Before placing the compartments in the incubators, two pumps need to be hooked up for constant flow of medium. This is done to account for evaporation of the medium keeping the V_f stable. After printing the cells must be examined daily to monitor cell growth.

2.2.9 Protocol cell culture

SMC and HUVECs were used in cell experiments. They were obtained from cryogenic storage from which they were thawed, seeded and left in culture for 7 days. Proper flasks were used so the correct amount of cells were obtained. When 80% confluence was achieved they were seeded and used for the bio-ink, spheroid culture and a new passage of cells. The following protocols were used for thawing and seeding of cells.

Thawing of cells

1. Remove the cryovial containing the frozen cells from liquid nitrogen storage and immediately place it into a 37°C water bath
2. Quickly thaw the cells (i 1 minute) by gently swirling the vial in the 37°C water bath until there is just a small bit of ice left in the vial
3. Transfer the vial into a laminar flow hood. Before opening, wipe the outside of the vial with 70% ethanol
4. Transfer the desired amount of pre-warmed complete growth medium appropriate for the required cell line dropwise into the tube containing the thawed cells
5. Gently suspend the cells (mixture of freezing medium and fresh pre-warmed medium) in complete growth medium (final dilution at least 1:20) and transfer them into the appropriate culture vessel and into the recommended culture environment (spread evenly)
6. Optional: After 3-4 hours (after survived cells attached to the plate) change medium

Seeding and counting of cells

1. Remove the medium and add an appropriate volume of Trypsin-EDTA (0,25 %)
2. Put the cells 3min in the incubator and after that gently tap the well plate to detach the cells
3. Centrifuge the cell suspension 3min at 300 x g (1000 rpm) at 4°C and remove supernatant (Trypsin-EDTA) without disturbing the cell pellet
4. Suspend the cells in 1 mL pre-warmed complete medium required for that cell type
5. Take a Neubauer Counting chamber (hemacytometer) and breath from a close distance on the surface and put a glass cover slip on it and move it gently till it's not moveable any more
6. Mix 10 μ L of the cell suspension with 90 μ L Trypan blue (0,04 %)
7. Pipette 10 μ L of this mixture between the Counting chamber and the cover slip and take it under the microscope
8. Determine the number of living cells (white cells) inside the four squares in the corners of the big square
9. Total cell number in 1mL cell suspension = (Counted cells of 4 Squares : 4) * 10 (Dilution of cell suspension in Trypan blue) x 10.000 (dilution factor in Counting chamber)
10. Typically, the concentration range for a cell count with Neubauer chamber is between 250.000 cells / mL and 2,5 million cells / mL
11. Use the appropriate cell starting cell density + appropriate volume of pre-warmed medium for the next passage

2.2.10 Protocol spheroid culture

SMC-HUVEC spheroids were used as an extension of the cell culture experiments. After counting cells, 200.000 cells of each cell type were placed in an agarose mold specifically designed for spheroid culture. The protocols below describe the creation of the agarose molds and the culture of spheroids

Production of Agarose molds

1. dissolve Agarose 3%
2. pour immediately the boiling agarose solution into the PDMS molds (6-Well plate), close the well plate and put the plate into the centrifuge (1200 rpm x 1min) → pay attention for balance in centrifuge)
3. wait 30 min and remove under the flow bench the agarose mold with a spatula (clean with ethanol before) and place them into 12-well plates
4. coat agarose molds with PBS, seal the plate with parafilm and store them in the fridge at 4°C

Spheroid production in agarose mold

1. add 200 μ L medium with $0,4 \cdot 10^6$ cells and let the cells settle down for 15min after that add 1,8 mL medium
2. after 24 h cells are fused to spheroids (approx. 267 cells/ spheroid)
3. every day half medium change till spheroid compaction is finished
4. flush out the spheroids with medium while the well plate is tilted (don't scratch with the pipet tip into the agarose otherwise fragments will be created)
5. Centrifuge 2200 rpm , 1 min

Chapter 3

Results

3.1 The characterization of Cytodex

The first milestone of this research is to specify the properties of Cytodex-3 microbeads. To determine the V_f of the suspension, average bead diameter, density and amount of beads per gram cytodex needed to be found. Density and amount of beads are stated in the literature [25] and for the average bead diameter two conditions were tested: A partly saturated and a fully saturated condition.

3.1.1 Partly saturated

As mentioned before, Cytodex-3 is a dry powder that expands upon contact with liquid. Due to this, the particles do not have a constant diameter. Cytodex-3 beads expand when more water is added until the point that they reach their maximum diameter. Assumed is that during this state the particles remain in tight packing at a V_f of 74%. After the point that particles have reached their maximum size the V_f will change. Because they are very clumped up it's hard to pin down the diameter of these beads. It is however very important to determine the diameter of fully expanded Cytodex-3 particles when working with volume fractions.

3.1.2 Fully saturated

To determine the average bead diameter in a fully saturated condition a 6 well plate was filled with a small amount of Cytodex-3 (< 1 mg) which was then filled with 2 mL of milli-Q. Different light-filters were tested which can be seen in figure 3.1 and 3.2.

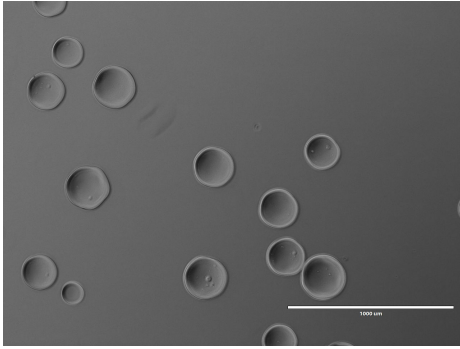


Figure 3.1: Highly diluted cytodex particles with high contrast

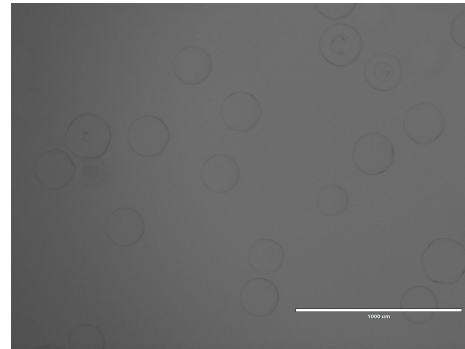


Figure 3.2: Highly diluted cytodex particles with low contrast

Figure 3.1 yielded the best results due to higher contrast. From these images, a mean diameter of $212 \pm 23\mu\text{m}$ was found for $n = 176$. A plot of the size distribution can be found in 3.3. The polydispersity was found at 0.54.

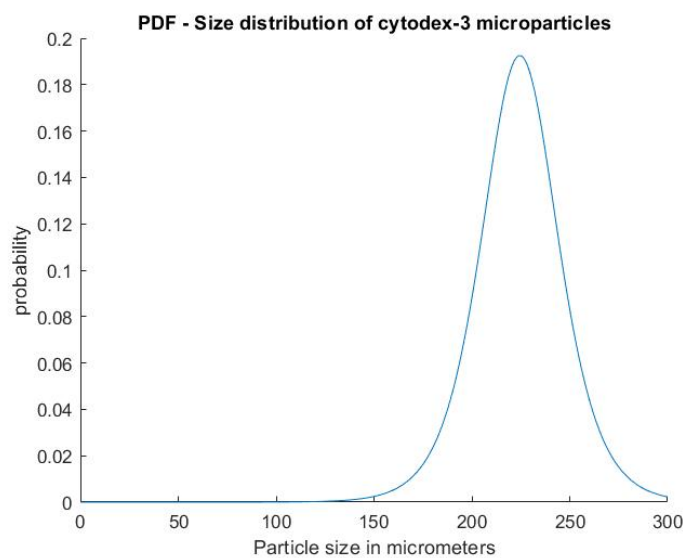


Figure 3.3: Size distribution of microparticles

3.2 Volume fraction and 3D printing: Establishing the operational window

Having determined the properties of Cytodex-3 this information can be used to calculate and experiment with the embedding baths using the V_f as a sole changing parameter. In this chapter, a range of suspensions with different volume fractions will be covered starting at 50% up to 70%. Not only the operational window for 3D printing will need to be determined, also the macro and micro effects of the Cytodex-3 suspension will be reviewed when we gradually increase the V_f .

3.2.1 Different volume fractions: Macro vs. Micro

First macro images of these volume fractions will be compared. Figure 3.4 shows how the embedding bath looks with a V_f of 50% and 55%. The biggest difference can be seen in the phase, whereas in the case of a low V_f the embedding bath behaves like a liquid when tilting the bio-reactor and for a high V_f the embedding bath does not. Figure 3.5 shows a V_f of 65% and 70%. One thing to note was that when the volume fraction was raised, the number of bubbles also increased. These are the white spots in the suspension.

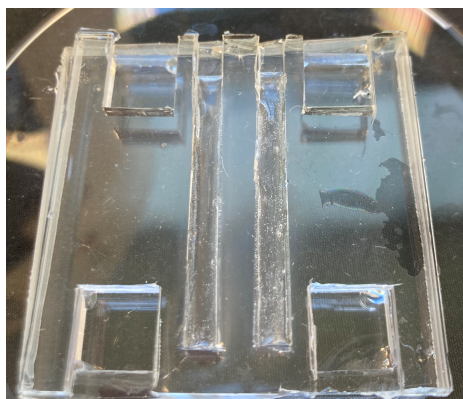


Figure 3.4: Macro image of suspensions with V_f 50%(L) and 55%(R)

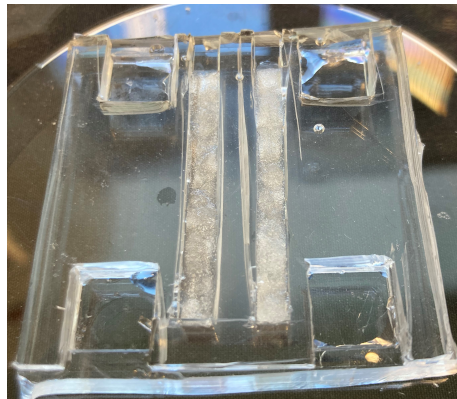


Figure 3.5: Macro image of suspensions with V_f 65%(L) and 70%(R)

The best way to capture the properties of the embedding baths is via microanalysis. This is done as described in subsection 2.2.6. The result of an embedding bath with $54 \pm 2\%$ is shown in figure 3.6. Due to the low V_f , a lot of interstitial liquid is present allowing the particles to move freely.

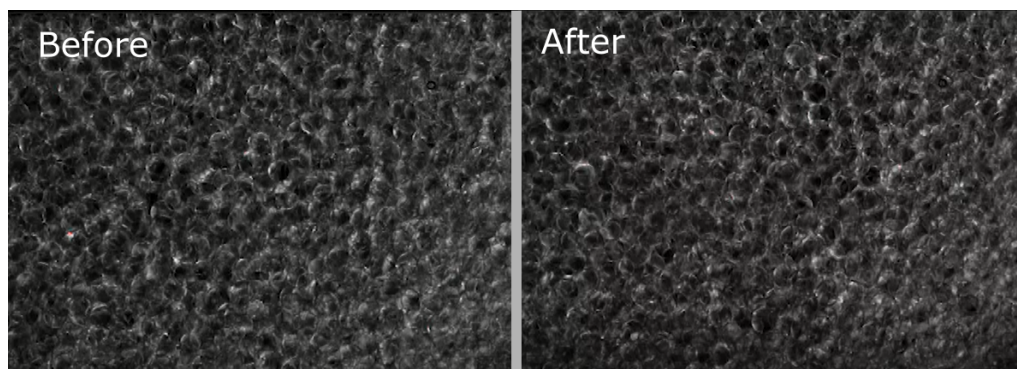


Figure 3.6: Before/After picture at 54% V_f

When the V_f is too high it loses its self-healing property which is illustrated in figure 3.7. The needle went diagonally through the embedding bath leaving a trail in its wake.

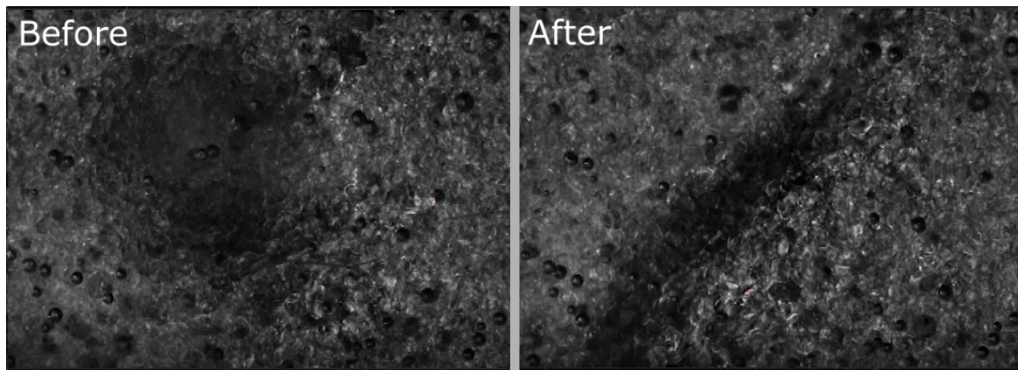


Figure 3.7: Before/After picture at 72% V_f

Figure 3.8 shows a V_f that is presenting the self-healing properties that are hoped to be achieved. Especially on the edges of the pictures, there are points of recognition, which means that locally the needle fluidized the embedding bath, but the global state of the embedding bath remains solid-like.

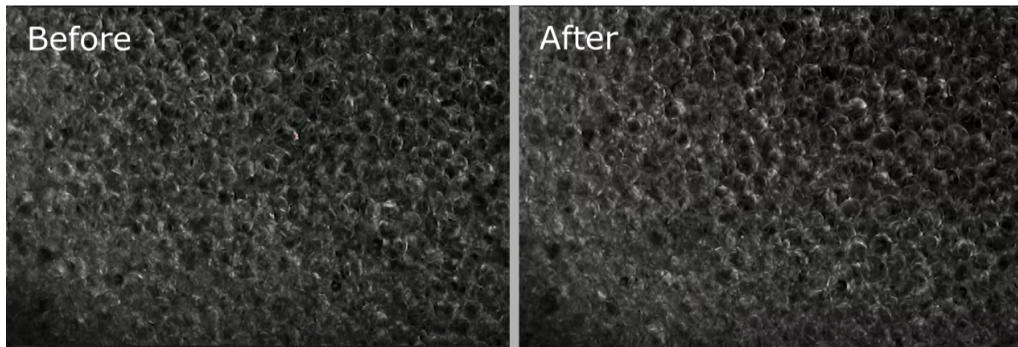
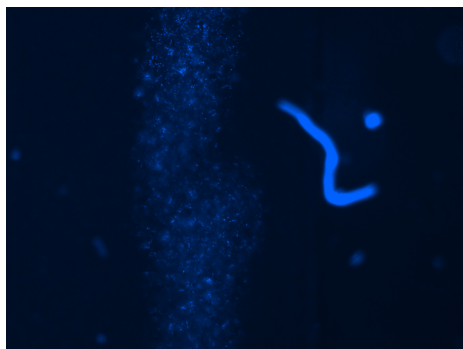
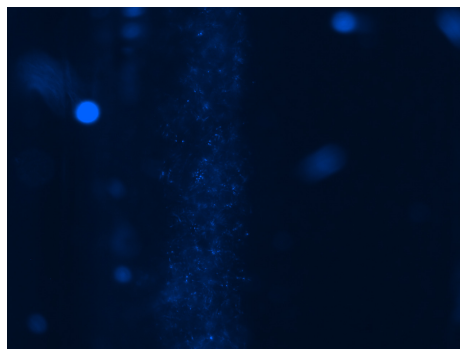


Figure 3.8: Before/After picture at 64% V_f

3.2.2 Determining print resolutions

To investigate print resolution in different V_f , an ink with 1.5 % (w/v) xanthan gum filled with transparent ultramarine blue airbrush color (Createx Colors) was used. All prints are done with the same G-code for consistency which can be found in Appendix B. The code constituted of a straight line through both compartments. The nozzle which was used for every print has an inner diameter of 410 μm . The goal is to find a V_f where the line that is printed has a width of approximately the same size as the nozzle. The expectation is that for low V_f the particles will move too freely and therefore can not keep the ink in place, which consequently will make the line too wide. For high V_f the nozzle will deform the embedding bath meaning it can not place the ink properly in the suspension.

In figure 3.9 a line can be observed which is printed in a suspension with a V_f of $52 \pm 2\%$. The line is not consistent in width and after analyses with imageJ the average print resolution was found at $980 \mu\text{m}$ with a minimum width of $793 \mu\text{m}$ and a maximum width of $1253 \mu\text{m}$. The range is as expected very high and the average is almost twice the nozzle size.

Figure 3.9: Printed line with 52% V_f Figure 3.10: Printed line with 60% V_f

The next figure (3.10) shows a line which is printed in a suspension with a V_f of $60 \pm 2\%$. The line is more consistent and also has a better resolution. The print resolution was found at an average of $677 \mu\text{m}$ with widths ranging from $557 \mu\text{m}$ to $789 \mu\text{m}$. So not only the average resolution has improved but with a range of approximately $200 \mu\text{m}$, the range has also decreased a tremendous amount.

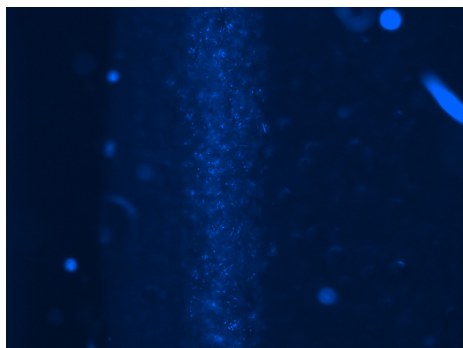
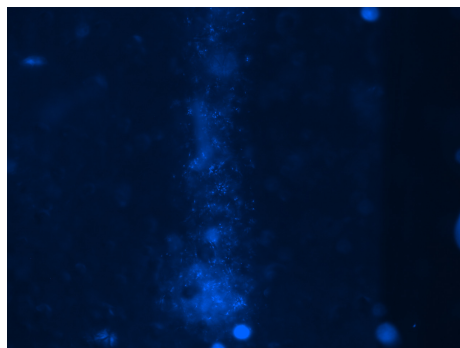
Figure 3.11: Printed line with 65% V_f Figure 3.12: Printed line with 70% V_f

Figure 3.11 and 3.12 shows lines printed in suspension with V_f of $65 \pm 2\%$ and $70 \pm 2\%$ respectively. The first figure has an average print resolution of $531 \mu\text{m}$. This was also the best print made during this thesis. The line was very consistent with a range of $445 \mu\text{m}$ to $619 \mu\text{m}$. Figure 3.12 shows an inconsistent distribution of particles because it lost its self-healing properties. For this reason, print resolutions were not found.

3.2.3 Print resolution vs. Volume fraction

To summarize the results found in subsection 3.2.2 a plot is generated where the print resolution is compared against the different volume fractions. The result can be seen in figure 3.13 and 3.14. Figure 3.13 shows the absolute value of the printed line. Figure 3.14 displays the line width related to the print nozzle. As you can be seen, for low V_f the line is almost twice as wide and the best results were found of a width 1.3 times the size of the inner diameter. The line is cut off from a V_f of 65% because no measurable results were obtained for higher V_f .

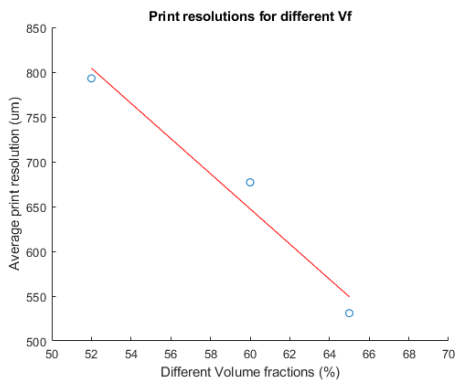


Figure 3.13: Absolute print resolution of different V_f

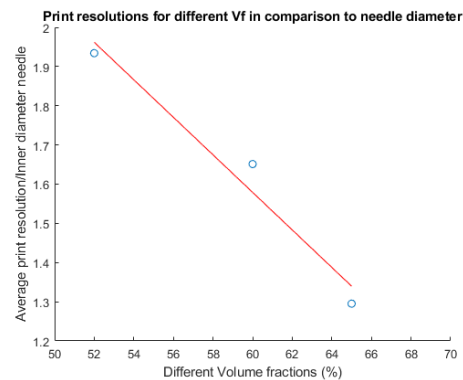


Figure 3.14: Print resolution related to the inner diameter of the nozzle

3.2.4 The complete line

To illustrate the whole compartment Inkscape was used to merge multiple microscopic pictures. This line is shown in 3.15 and is very consistent apart from one discontinuation. This is probably due to bubbles in the syringe since no material seems to be extruded outside of the line trajectory.

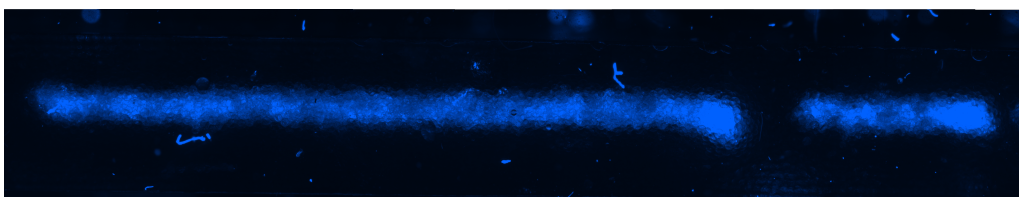


Figure 3.15: Merged picture of the full line

3.3 Cell printing

During this thesis, there have been two tries of cell printing and one try of spheroid printing was performed. At the moment of printing, the amount of HUVECs were limited therefore the ratio SMC:HUVEC was changed to 4:1. During testing, the medium for the embedding baths was never exposed outside of the LAF-cabinet to lower the chance of infections. Since the cell printing experiments were rather early in the experimental phase and the extra challenge of preparing the embedding baths in a sterile environment no results are yet to be obtained. It is however shown in experiments done by Vincent Rangel, that it is possible to print the cell-laden bio-ink and keep cells embedded in the granular medium.

Spheroid printing was performed after spheroids were cultured. Due to low amounts of spheroids that were put in the ink in comparison to the total volume the chance of printing spheroids became very slim. After printing several times in the embedding baths still no spheroids were observed in the granular medium. Unfortunately this means that no results can be shown in this section.

Chapter 4

Discussion

Through the process of finding the operational window of printing in a Cytodex-3 embedding bath, there were a few problems that will be addressed in this chapter. These problems need to be taken into consideration when continuing with future experiments.

First of all, it is hard to accurately estimate the V_f using the method of the stock solution. This is because when extruding the Cytodex-3, it was hard to accurately extrude the right amount of Cytodex-3 in the compartments. Because of the high number of beads in just a little amount of stock solutions, errors become very large very quickly. A solution to this problem is using a balance inside a sterile environment to directly place the Cytodex-3 inside the compartments before adding liquid. By doing this, it is easier to maintain control over the number of beads added and therefore the V_f can be estimated more accurately.

Before every print, the needle needs to be calibrated in the z-direction. This introduced human error into the process because this had to be done by hand. If the needle is calibrated too high the ink was not visible through the microscope. On the other hand, if the needle was calibrated too low it would shatter the glass plate used for microscopy. Standardizing this process is a way to overcome this problem. Solutions to this process would be laser-guided calibration or making sure that the bed level of the print is always at the same height.

Evaporation is something to always take into consideration because of the high surface area of the particles. The evaporation rate was found at approximately 0.1 mg/s. This made the print window rather short because after a few hours V_f started to rise, making it impossible to maintain a constant V_f . When cell experiments are started this needs to be overcome by attaching a pump to the embedding bath for constant flow.

There was a correlation between the number of bubbles in the embedding bath and the V_f . If the V_f rose, so did the bubbles. This is probably because the particles could more easily 'capture' the bubbles when becoming more dominant in the suspension. Vacuum the embedding baths was tried but had little effect. Eventually, to minimize hindrance the bigger bubbles were removed by hand with a needle while the smaller bubbles were hardly visible under the microscope.

When looking at the complete line, sometimes there were gaps present. These gaps seemed to appear random. Since no materials were extruded outside of the line trajectory, the probable cause was bubbles inside the syringe. To bypass this, the syringe has to be loaded before every print as well as careful handling when loading the syringe.

During the course of this thesis, one print was done with spheroid-laden bio-ink. Although many prints were done in the same embedding bath no spheroids were seen under the microscope. This was probably because of the low V_f of the spheroids in the bio-ink. This made the chance of a spheroid being printed very low. Whilst printing this was tried to be overcome by printing multiple times into the same compartment, without any luck. This is not the best solution to the problem since each print lowers the V_f of the embedding bath. A better solution would be to raise the V_f of spheroids inside the bio-ink to a maximum of 10% V_f . This number is chosen because in this particular situation there is little to no interaction between the spheroids inside the bio-ink [35].

Chapter 5

Conclusion

In the introduction, four milestones were set to create a 2,5D environment for vascularization. These four points were:

1. The characterization of the cytodex microbeads
2. Finding the operational window for printing
3. Printing of cells in a Cytodex-3 microbead suspension
4. Printing of spheroids in a Cytodex-3 microbead suspension

Due to time restrictions, only the first two milestones were completed, but a path has been paved to continue experimenting with cells.

Cytodex-3 proved to be an excellent microparticle for creating a stable embedding bath. During characterization of the Cytodex-3 beads, the average diameter was found at $212 \mu\text{m}$ with a polydispersity of 0.54. Although it was not determined exactly, it can be assumed that during the growth of the cytodex beads the V_f stays stable at approximately 74% (tight packing), until it reaches its max diameter of approximately $212 \pm 26 \mu\text{m}$. From this point onward the diameter will be more or less constant whilst the V_f changes because of an increase in interstitial liquid.

Looking at the microscopic pictures and the print resolution, we can conclude that the V_f as the sole parameter is a great way to influence the behavior of the different embedding baths. When using a lower fraction, the ink is able to move too freely in the suspension causing the line to be wider than desired. When using a higher fraction, the suspension loses its self-healing property, which in turn makes the needle destroy the embedding bath. The operational window was found at V_f between 60% and 65%. Best print resolutions were found at a V_f of 65% with a print width to nozzle ratio of 1.3.

The next step is to start cell experiments. Due to the nature of Cytodex-3, the hypothesis is that it has a high potential to be successfully used as an embedding bath for cell culture.

Bibliography

- [1] Patrick Holzmann et al. *User entrepreneur business models in 3D printing*. 2017. DOI: 10.1108/JMTM-12-2015-0115.
- [2] J. P. Kruth. “Material Incess Manufacturing by Rapid Prototyping Techniques”. In: *CIRP Annals - Manufacturing Technology* 40.2 (Jan. 1991), pp. 603–614. ISSN: 17260604. DOI: 10.1016/S0007-8506(07)61136-6.
- [3] N. Shahrubudin, T. C. Lee, and R. Ramlan. “An overview on 3D printing technology: Technological, materials, and applications”. In: *Procedia Manufacturing*. Vol. 35. Elsevier B.V., 2019, pp. 1286–1296. DOI: 10.1016/j.promfg.2019.06.089.
- [4] Sean V. Murphy and Anthony Atala. *3D bioprinting of tissues and organs*. Aug. 2014. DOI: 10.1038/nbt.2958. URL: <https://www.nature.com/articles/nbt.2958>.
- [5] Heqi Xu, Jazzmin Casillas, and Changxue Xu. “Effects of printing conditions on cell distribution within microspheres during inkjet-based bioprinting”. In: *AIP Advances* 9.9 (Sept. 2019), p. 095055. ISSN: 21583226. DOI: 10.1063/1.5116371. URL: <https://doi.org/10.1063/1.5116371>.
- [6] Dafydd O. Visscher et al. *Advances in Bioprinting Technologies for Craniofacial Reconstruction*. Sept. 2016. DOI: 10.1016/j.tibtech.2016.04.001.
- [7] Ibrahim T. Ozbolat and Monika Hospodiuk. *Current advances and future perspectives in extrusion-based bioprinting*. Jan. 2016. DOI: 10.1016/j.biomaterials.2015.10.076.
- [8] Nityananda Sahoo et al. *Recent advancement of gelatin nanoparticles in drug and vaccine delivery*. Nov. 2015. DOI: 10.1016/j.ijbiomac.2015.08.006.
- [9] Christian Mandrycky et al. *3D bioprinting for engineering complex tissues*. July 2016. DOI: 10.1016/j.biotechadv.2015.12.011.
- [10] Rebecca E. Taylor et al. “Sacrificial layer technique for axial force post assay of immature cardiomyocytes”. In: *Biomedical Microdevices* 15.1 (Feb. 2013), pp. 171–181. ISSN: 13872176. DOI: 10.1007/s10544-012-9710-3. URL: <https://link.springer.com/article/10.1007/s10544-012-9710-3>.
- [11] Jordan S. Miller et al. “Rapid casting of patterned vascular networks for perfusable engineered three-dimensional tissues”. In: *Nature Materials* 11.9 (July 2012), pp. 768–774. ISSN: 14764660. DOI: 10.1038/nmat3357. URL: www.nature.com/naturematerials.
- [12] Thomas J. Hinton et al. “Three-dimensional printing of complex biological structures by freeform reversible embedding of suspended hydrogels”. In: *Science Advances* 1.9 (Oct. 2015), e1500758. ISSN: 23752548. DOI: 10.1126/sciadv.1500758. URL: <http://advances.sciencemag.org/>.
- [13] Tapomoy Bhattacharjee et al. “Writing in the granular gel medium”. In: *Science Advances* 1.8 (Sept. 2015), e1500655. ISSN: 23752548. DOI: 10.1126/sciadv.1500655. URL: <http://advances.sciencemag.org/>.

-
- [14] N. C. Rivron et al. *Engineering vascularised tissues in vitro*. 2008. DOI: 10.22203/eCM.v015a03.
- [15] Scott A. Rodeo et al. “2011 aoa symposium: Tissue engineering and tissue regeneration: Aoa critical issues”. In: *Journal of Bone and Joint Surgery - Series A*. Vol. 95. 15. Journal of Bone and Joint Surgery Inc., Aug. 2013. DOI: 10.2106/JBJS.K.01505.
- [16] Hassan K. Awwad et al. “Intercapillary distance measurement as an indicator of hypoxia in carcinoma of the cervix uteri”. In: *International Journal of Radiation Oncology, Biology, Physics* 12.8 (1986), pp. 1329–1333. ISSN: 03603016. DOI: 10.1016/0360-3016(86)90165-3. URL: <https://pubmed.ncbi.nlm.nih.gov/3759554/>.
- [17] Ying Chieh Chen et al. “Functional human vascular network generated in photocrosslinkable gelatin methacrylate hydrogels”. In: *Advanced Functional Materials* 22.10 (May 2012), pp. 2027–2039. ISSN: 1616301X. DOI: 10.1002/adfm.201101662. URL: www.MaterialsViews.com.
- [18] Marina I. Santos and Rui L. Reis. *Vascularization in bone tissue engineering: Physiology, current strategies, major hurdles and future challenges*. Jan. 2010. DOI: 10.1002/mabi.200900107. URL: www.mbs-journal.de.
- [19] Kayla Duval et al. *Modeling physiological events in 2D vs. 3D cell culture*. June 2017. DOI: 10.1152/physiol.00036.2016. URL: www.physiologyonline.org.
- [20] Anna Birgersdotter, Rickard Sandberg, and Ingemar Ernberg. *Gene expression perturbation in vitro - A growing case for three-dimensional (3D) culture systems*. Oct. 2005. DOI: 10.1016/j.semcan.2005.06.009.
- [21] Megan E. Smithmyer, Samantha E. Cassel, and April M. Kloxin. “Bridging 2D and 3D culture: Probing impact of extracellular environment on fibroblast activation in layered hydrogels”. In: *AIChE Journal* 65.12 (Dec. 2019). ISSN: 15475905. DOI: 10.1002/aic.16837.
- [22] Swati Pradhan-Bhatt et al. “Implantable three-dimensional salivary spheroid assemblies demonstrate fluid and protein secretory responses to neurotransmitters”. In: *Tissue Engineering - Part A* 19.13-14 (July 2013), pp. 1610–1620. ISSN: 1937335X. DOI: 10.1089/ten.tea.2012.0301. URL: www.liebertpub.com.
- [23] Aswin Sundarakrishnan et al. *Engineered cell and tissue models of pulmonary fibrosis*. Apr. 2018. DOI: 10.1016/j.addr.2017.12.013.
- [24] Mark Phillip Pebworth, Sabrina A. Cismas, and Prashanth Asuri. “A novel 2.5D culture platform to investigate the role of stiffness gradients on adhesion-independent cell migration”. In: *PLoS ONE* 9.10 (Oct. 2014), e110453. ISSN: 19326203. DOI: 10.1371/journal.pone.0110453. URL: <https://doi.org>.
- [25] gelifesciences.com. Tech. rep.
- [26] *Dr. INVIVO 4D2* — ROKIT Healthcare, INC. URL: <https://rokithealthcare.com/invivo/>.
- [27] Marijn M. Kool et al. “The influence of the primary and secondary xanthan structure on the enzymatic hydrolysis of the xanthan backbone”. In: *Carbohydrate Polymers* 97.2 (Sept. 2013), pp. 368–375. ISSN: 01448617. DOI: 10.1016/j.carbpol.2013.05.045.
- [28] Indu Sara Benny, V Gunasekar, and V Ponnusami. *Review on Application of Xanthan Gum in Drug Delivery*. Tech. rep. 4, pp. 1322–1326.
- [29] Mahmoud H. Abu Elella et al. *Xanthan gum-derived materials for applications in environment and eco-friendly materials: A review*. Feb. 2021. DOI: 10.1016/j.jece.2020.104702.

- [30] *Comprehensive Microsystems — ScienceDirect*. URL: <https://www.sciencedirect.com/referencework/9780444521903/comprehensive-microsystems>.
- [31] Diana J. Medina-Leyte et al. “Use of Human Umbilical Vein Endothelial Cells (HUVEC) as a Model to Study Cardiovascular Disease: A Review”. In: *Applied Sciences* 2020, Vol. 10, Page 938 10.3 (Jan. 2020), p. 938. DOI: 10.3390/APP10030938. URL: <https://www.mdpi.com/2076-3417/10/3/938/htm%20https://www.mdpi.com/2076-3417/10/3/938>.
- [32] T Maciag et al. “Serial propagation of human endothelial cells in vitro.” In: *Journal of Cell Biology* 91.2 (Nov. 1981), pp. 420–426. ISSN: 0021-9525. DOI: 10.1083/JCB.91.2.420. URL: <http://rupress.org/jcb/article-pdf/91/2/420/1075357/420.pdf>.
- [33] Sarah K. Steinbach and Mansoor Husain. “Vascular smooth muscle cell differentiation from human stem/progenitor cells”. In: *Methods* 101 (May 2016), pp. 85–92. DOI: 10.1016/J.YMETH.2015.12.004.
- [34] *Density Gradient Media and Centrifugation Overview*. URL: <https://www.stemcell.com/density-gradient-media-overview.html>.
- [35] Jan Mewis and Norman J. Wagner. “Colloidal Suspension Rheology- Jan Mewis and Norman J. Wagner.pdf”. In: *Cambridge University Press* (2012), p. 393.
- [36] M. Pica Ciamarra, A. Coniglio, and A. De Candia. “Disordered jammed packings of frictionless spheres”. In: *Soft Matter* 6.13 (July 2010), pp. 2975–2981. ISSN: 1744683X. DOI: 10.1039/c001904f. URL: www.rsc.org/softmatter.
- [37] Todd M. Squires and John F. Brady. “A simple paradigm for active and nonlinear microrheology”. In: *Physics of Fluids* 17.7 (2005), pp. 1–21. DOI: 10.1063/1.1960607.

Appendix A

Abstract Nederlands

Vanwege de laatste ontwikkelingen in 3D bioprinting wordt het maken van grotere biologische structuren steeds meer een realiteit. Dit brengt echter een probleem met zich mee, het maken van vasculair weefsel. In dit onderzoek is gebruik gemaakt van een nieuwe 3D bioprint techniek die gebruik maakt van het printen in een Cytodex-3 suspensie. Door de karakteristieken van deze microparticle suspensie wordt er een 2,5D cell kweek omgeving gecreëerd om vascularizatie te stimuleren. De parameter die het gedrag van deze suspensie bepaald is de Volume fraction (V_f) en wordt gedefinieerd als het volume wat de microparticles innemen van het totaal volume. Het doel van het onderzoek is het vinden van de ideale V_f om in te printen. Om dit te bewerkstelllen worden de Cytodex-3 microparticles eerst gekarakteriseerd, vervolgens worden suspensies met V_f van 50% tot 70% geanalyseerd op macro en micro schaal. Daarna wordt er gekeken welke V_f de beste printresultaten geven. De laatste stap zal zijn om met Human Umbilical Vein Endothelial Cells (HUVECs) en Smooth Muscle Cells (SMCs) single cells and spheroids te printen in een suspensie met de ideale V_f . Resultaten laten zien dat de Cytodex-3 microparticles bolvormig zijn met een gemiddelde diameter van $212 \mu\text{m}$ en een polydispersity van 0.54. Het printwindow bleek groot te zijn met een V_f van 55% tot 65%. Bij hogere V_f verloor de suspensie zijn zelf genezende eigenschappen. Alle prints zijn gemaakt met een naald met een diameter van $410 \mu\text{m}$. Print resultaten worden daarom ook gemeten met deze diameter. De beste print resultaten waren gevonden op $677 \pm 120 \mu\text{m}$ en $531 \pm 90 \mu\text{m}$ voor 60% en 65% respectievelijk. Vanwege tijd restricties is het nog niet gelukt om met cellen te printen, maar gezien de veelbelovende resultaten is dit zeker aan te raden.

Appendix B

G-code

The G-code used in this assignment was granted and made by BSc Vincent Rangel

```
G21; set units to mm,
G90; set positioning to absolute,
M104 S35 T0 (set extruder temperature)
G92 Z0
G1 Z20 F120
G28 X Y F1000 (home XY axes maximum)
G28 Z F120 (home Z axis minimum)
M1010 S1
G95 P2
;G1 Z20 F1500
;G1 X32 Y17 F1500
;M109 S35 T0 ;wait for extruder to reach temperature
;M106 P4 S255 ;uv led1
;M106 P3 S255 ;uv led2
M1015 P1 F60.0 E-0.5
G92 E0 (Set E to 0 again)
T2 ;Switch to the first extruder
;**** end of start-gcode ****)
;Edislicer 3.7.29 (Aug 16 2019 08:55:27)
;config.smallSkinSpeedHalfInfillSpeed = 0 20
;Nozzle1:infill line-width(NozzleSize) = 0.4(0.4)
;Nozzle2:infill line-width(NozzleSize) = 0.4(0.4)
;Nozzle3:infill line-width(NozzleSize) = 0.4(0.4)
;
G1 Z25.000 F900 (Nozzle Hop)
G0 F1200 X85.700 Y82.490
;Layer count: 1
M73 P0 ( LAYER: 1 )
;LAYER:1
M106 S255 (Fan On)
27
B.1 G-code
;G1 F60 E-0.20000 (Nozzle Switch retraction)
G92 E0
G1 Z25.000 F600 H1(Nozzle Switch Hop5)
;
```

```
;(TOOL CHANGE6)
T1
;
;Block 1
M203 Z7 ;Z axis max speed 7 mm/sec
G1 Z0.200 F600
G1 F600 X85.700 Y74.690 E0.08000
G1 X85.700 Y50.490 E0.30315 ;right channel
G92 E0
M73 P50
G1 Z20.000 F600 H1(Nozzle Switch Hop5)
G1 Z20.000 F600
G0 F1200 X76.300 Y82.490
G92 E0.00000 (Nozzle Switch back-retraction2)
G1 F60 E0 (Nozzle Switch back-retraction2)
G1 Z0.200 F600
G1 F60 E0.00000 (Back-retraction)
G1 F600 X76.300 Y74.690 E0.08000
G1 X76.300 Y50.490 E0.30315 ;left channel
G92 E0
M73 P100
;G1 F60 E-0.10000 (Nozzle retraction)
G1 Z3.300 F600 (Nozzle Hop)
M73 P100 ( LAYER: 2 )
;LAYER:2
;
;**** start of end-gcode for Edison Bio NK 1.57.68.0 BI-P1-01-170320-0010 ****)
M73 P100 ; end progress
```